

Acoustics in lined ducts with sheared mean flow, with applications for aircraft noise

Sjoerd Rienstra & Martien Oppeneer

with major contributions from

Pieter Sijtsma, Bob Mattheij, Werner Lazeroms

TU/e, 31 March 2015

Summary

- Acoustic modes in flow ducts, with radial mean flow and temperature gradients.

Summary

- Acoustic modes in flow ducts, with radial mean flow and temperature gradients.
- Boundary condition (Helmholtz resonator-type) varies axially.

Summary

- Acoustic modes in flow ducts, with radial mean flow and temperature gradients.
- Boundary condition (Helmholtz resonator-type) varies axially.
- Mode matching works well for uniform flow, but here?

Summary

- Acoustic modes in flow ducts, with radial mean flow and temperature gradients.
- Boundary condition (Helmholtz resonator-type) varies axially.
- Mode matching works well for uniform flow, but here?
- **Slowly-varying mode approximation** works well if Z not passing resonance.

Summary

- Acoustic modes in flow ducts, with radial mean flow and temperature gradients.
- Boundary condition (Helmholtz resonator-type) varies axially.
- Mode matching works well for uniform flow, but here?
- **Slowly-varying mode approximation** works well if Z not passing resonance.
- Efficient and accurate **new Mode-Matching method** based on **exact** integrals of modes.

Summary

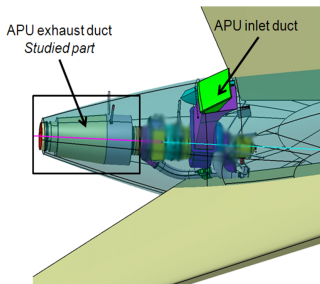
- Acoustic modes in flow ducts, with radial mean flow and temperature gradients.
- Boundary condition (Helmholtz resonator-type) varies axially.
- Mode matching works well for uniform flow, but here?
- **Slowly-varying mode approximation** works well if Z not passing resonance.
- Efficient and accurate **new Mode-Matching method** based on **exact** integrals of modes.

Published in: AIAA-2011-2871, AIAA-2013-2172.

- 1 Background & motivation
- 2 Pridmore-Brown modes
- 3 Options for varying Z
- 4 WKB for slowly varying Z
- 5 New mode-matching method
- 6 Conclusions

- 1 Background & motivation
- 2 Pridmore-Brown modes
 - Model & equations
 - Numerical method: COLNEW and path-following
- 3 Options for varying Z
- 4 WKB for slowly varying Z
- 5 New mode-matching method
 - Mode-matching basics
 - Closed-form integrals of Helmholtz modes
 - Closed-form integrals of radial Pridmore-Brown modes
 - Mode-matching based on closed form integrals of PB modes
 - Numerical results: comparing CMM and BLM
- 6 Conclusions
 - Epilogue

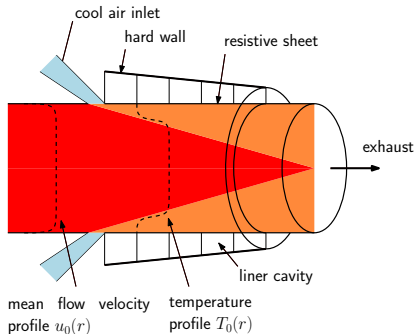
- APU: Auxiliary Power Unit
 - produces power when main engines are switched off
 - to start main engines, AC, ...
 - **major source of ramp noise**



APU on an Airbus A380

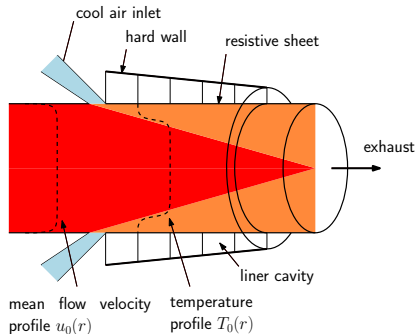
Study sound propagation & attenuation in APU exhaust duct.

Modelling assumptions



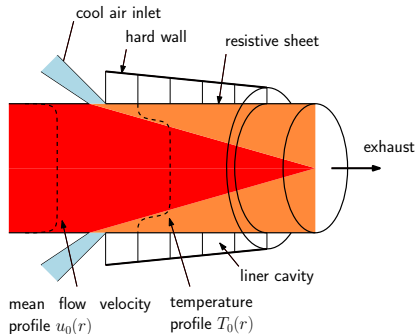
- straight, circular, hollow exhaust duct

Modelling assumptions



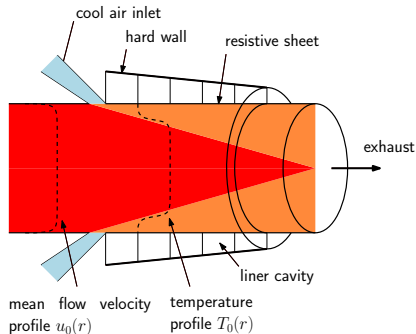
- straight, circular, hollow exhaust duct
- non-uniform parallel mean flow (~~axially varying~~)

Modelling assumptions



- straight, circular, hollow exhaust duct
- non-uniform parallel mean flow (~~axially varying~~)
- strong temperature gradients (~~axially varying~~)

Modelling assumptions



- straight, circular, hollow exhaust duct
- non-uniform parallel mean flow (~~axially varying~~)
- strong temperature gradients (~~axially varying~~)
- segmented liner \Rightarrow slowly varying or mode-matching
- Euler eqn. & perfect gas: $p = \rho \mathcal{R} T$, $c^2 = \gamma \mathcal{R} T$

- 1 Background & motivation
- 2 Pridmore-Brown modes
 - Model & equations
 - Numerical method: COLNEW and path-following
- 3 Options for varying Z
- 4 WKB for slowly varying Z
- 5 New mode-matching method
 - Mode-matching basics
 - Closed-form integrals of Helmholtz modes
 - Closed-form integrals of radial Pridmore-Brown modes
 - Mode-matching based on closed form integrals of PB modes
 - Numerical results: comparing CMM and BLM
- 6 Conclusions
 - Epilogue

Ordinary & Generalised Pridmore-Brown equation

For perturbations $p_1, \rho_1, \mathbf{v}_1$ of a parallel mean flow

$$\mathbf{v}_0 = u_0(y, z)\mathbf{e}_x, \quad \rho_0 = \rho_0(y, z), \quad c_0 = c_0(y, z), \quad p_0 = \text{const}$$

Ordinary & Generalised Pridmore-Brown equation

For perturbations p_1, ρ_1, v_1 of a parallel mean flow

$$v_0 = u_0(y, z)e_x, \quad \rho_0 = \rho_0(y, z), \quad c_0 = c_0(y, z), \quad p_0 = \text{const}$$

the Linearised Euler equations can be reduced to:

Generalised Pridmore-Brown equation (arbitrary cross-section)

For modes of the form $p_1(x, y, z, t) = P(y, z) e^{ikx - i\omega t}$:

$$\nabla \cdot \left(\frac{c_0^2}{\Omega^2} \nabla P \right) + \left(1 - \frac{k^2 c_0^2}{\Omega^2} \right) P = 0, \quad \Omega = \omega - k u_0$$

Ordinary & Generalised Pridmore-Brown equation

For perturbations p_1, ρ_1, v_1 of a parallel mean flow

$$v_0 = u_0(y, z)e_x, \quad \rho_0 = \rho_0(y, z), \quad c_0 = c_0(y, z), \quad p_0 = \text{const}$$

the Linearised Euler equations can be reduced to:

Generalised Pridmore-Brown equation (arbitrary cross-section)

For modes of the form $p_1(x, y, z, t) = P(y, z) e^{ikx - i\omega t}$:

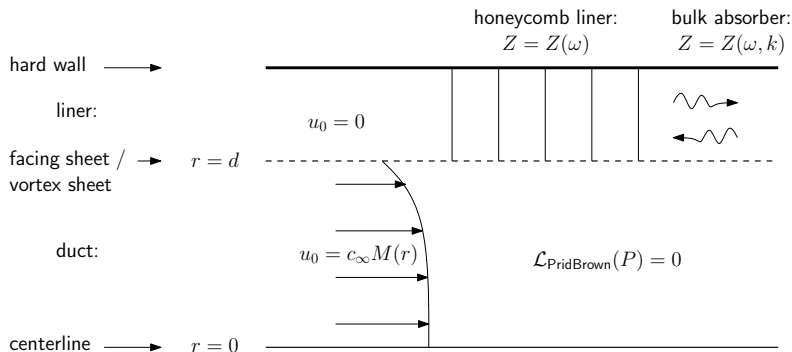
$$\nabla \cdot \left(\frac{c_0^2}{\Omega^2} \nabla P \right) + \left(1 - \frac{k^2 c_0^2}{\Omega^2} \right) P = 0, \quad \Omega = \omega - k u_0$$

Ordinary Pridmore-Brown equation (circular cross-section)

For $u_0(r), \rho_0(r), c_0(r)$ and $p_1(x, r, \theta, t) = P(r) e^{ikx - i\omega t + im\theta}$:

$$P'' + \left(\frac{1}{r} + 2 \frac{c_0'}{c_0} + 2 \frac{k u_0'}{\Omega} \right) P' + \left(\frac{\Omega^2}{c_0^2} - k^2 - \frac{m^2}{r^2} \right) P = 0$$

Boundary conditions



Ingard-Myers boundary condition for slipping flow:

$$-i\omega(\mathbf{v}_1 \cdot \mathbf{n})Z = (-i\omega + \mathbf{v}_0 \cdot \nabla)p_1$$

Boundary value problem

Pridmore-Brown equation

$$P'' + \left(\frac{1}{r} + 2\frac{c_0'}{c_0} + 2\frac{ku_0'}{\Omega} \right) P' + \left(\frac{\Omega^2}{c_0^2} - k^2 - \frac{m^2}{r^2} \right) P = 0$$

+

Boundary conditions

$$i\omega Z P' = -\rho_0 \Omega^2 P \quad \text{at } r = d, \quad P \text{ is regular at } r = 0$$

=

Eigenvalue Problem in k

Countable set of modal solutions: $P_{m\mu}(r) e^{ik_{m\mu}x - i\omega t + im\theta}$

- eigenfunctions: $P_{m\mu}(r)$
- eigenvalue (modal axial wavenumber): $k_{m\mu}$

Boundary value problem

Pridmore-Brown equation

$$P'' + \left(\frac{1}{r} + 2\frac{c_0'}{c_0} + 2\frac{ku_0'}{\Omega} \right) P' + \left(\frac{\Omega^2}{c_0^2} - k^2 - \frac{m^2}{r^2} \right) P = 0$$

+

Boundary conditions

$$i\omega Z P' = -\rho_0 \Omega^2 P \quad \text{at } r = d, \quad P \text{ is regular at } r = 0$$

=

Eigenvalue Problem in k

Countable set of modal solutions: $P_{m\mu}(r) e^{ik_{m\mu}x - i\omega t + im\theta}$

- eigenfunctions: $P_{m\mu}(r)$
- eigenvalue (modal axial wavenumber): $k_{m\mu}$

Non-uniform parallel flow: modes are found numerically

Write eigenvalue problem as boundary value problem:

- Add k to solution vector by adding equation $k' = 0$
- Fix $P(r)$ at $r = d$

Write eigenvalue problem as boundary value problem:

- Add k to solution vector by adding equation $k' = 0$
- Fix $P(r)$ at $r = d$

COLNEW (NL-BVP software package available on netlib):

- Collocation at Gaussian points
- Runge-Kutta monomial basis representation
- Automatic meshing
- Damped Newton solver

Write eigenvalue problem as boundary value problem:

- Add k to solution vector by adding equation $k' = 0$
- Fix $P(r)$ at $r = d$

COLNEW (NL-BVP software package available on netlib):

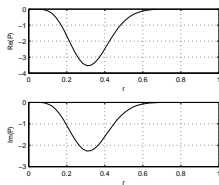
- Collocation at Gaussian points
- Runge-Kutta monomial basis representation
- Automatic meshing
- Damped Newton solver

Path-following/predictor-corrector/automatic step-size strategy from known solution to desired solution.

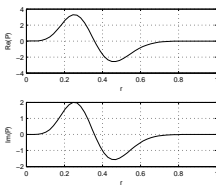
Numerical approach: example of path-following

Example of path-following in Z

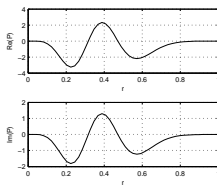
Numerical results: eigenfunctions & eigenvalues



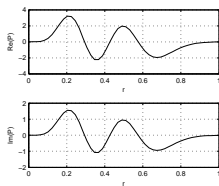
(a) $\mu = 1$



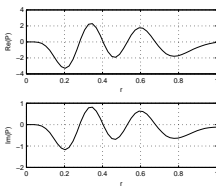
(b) $\mu = 2$



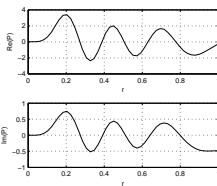
(c) $\mu = 3$



(d) $\mu = 4$



(e) $\mu = 5$



(f) $\mu = 6$

Eigenfunctions for upstream-running modes, $\omega d/c_\infty = 25$, $m = 5$,
 $Z/\rho_\infty c_\infty = 2 - i$, $u_0/c_\infty = \frac{2}{3}(1 - \frac{1}{2}r^2)$, uniform temperature.

Numerical results: further tests

Test case borrowed from quantum-mech. potential well problem:

- Pridmore-Brown equation:

$$P'' + \beta(r, k)P' + \gamma(r, k)P = 0$$

- *Quantisation condition* based on high-freq. approximation

$$\int_{r_1}^{r_2} \sqrt{\gamma(r, k)} dr = (n - \tfrac{1}{2})\pi, \quad n = 1, 2, \dots$$

μ	k_{QC}	k
1	-60.470038	-60.4392
2	-55.761464	-55.7281
3	-51.134207	-51.0980 - 0.0000i
4	-46.605323	-46.5659 - 0.0003i
5	-42.195790	-42.1422 - 0.0212i
6	-37.931052	-37.5622 - 0.3254i

k 's for upstream-running modes.

- High-freq. approx. & numerical result: excellent agreement

- 1 Background & motivation
- 2 Pridmore-Brown modes
 - Model & equations
 - Numerical method: COLNEW and path-following
- 3 Options for varying Z
- 4 WKB for slowly varying Z
- 5 New mode-matching method
 - Mode-matching basics
 - Closed-form integrals of Helmholtz modes
 - Closed-form integrals of radial Pridmore-Brown modes
 - Mode-matching based on closed form integrals of PB modes
 - Numerical results: comparing CMM and BLM
- 6 Conclusions
 - Epilogue

Options for varying Z

General solution by sum over modes

$$p_m(r, x) = \sum_{\mu=1}^{\mu^{\max}} \left[A_{m\mu}^+ P_{m\mu}^+(r) e^{ik_{m\mu}^+ x} + A_{m\mu}^- P_{m\mu}^-(r) e^{ik_{m\mu}^- x} \right]$$

Classic option for (piecewise) varying Z is *Mode Matching*.

Options for varying Z

General solution by sum over modes

$$p_m(r, x) = \sum_{\mu=1}^{\mu^{\max}} \left[A_{m\mu}^+ P_{m\mu}^+(r) e^{ik_{m\mu}^+ x} + A_{m\mu}^- P_{m\mu}^-(r) e^{ik_{m\mu}^- x} \right]$$

Classic option for (piecewise) varying Z is *Mode Matching*.

This is efficient and well-established (BAHAMAS ◀ NLR) for no-flow and uniform flow conditions, mainly because

- exact solutions of PB equation ($P_{m\mu} = J_m$ Bessel functions),
- exact modal inner products (integrals) at interfaces.

Options for varying Z

General solution by sum over modes

$$p_m(r, x) = \sum_{\mu=1}^{\mu^{\max}} \left[A_{m\mu}^+ P_{m\mu}^+(r) e^{ik_{m\mu}^+ x} + A_{m\mu}^- P_{m\mu}^-(r) e^{ik_{m\mu}^- x} \right]$$

Classic option for (piecewise) varying Z is *Mode Matching*.

This is efficient and well-established (BAHAMAS ◀ NLR) for no-flow and uniform flow conditions, mainly because

- exact solutions of PB equation ($P_{m\mu} = J_m$ Bessel functions),
- exact modal inner products (integrals) at interfaces.

Questions for non-uniform mean flow:

- What can we do with a *slowly* varying impedance?
- Can we improve the efficiency of the mode-matching?

- 1 Background & motivation
- 2 Pridmore-Brown modes
 - Model & equations
 - Numerical method: COLNEW and path-following
- 3 Options for varying Z
- 4 WKB for slowly varying Z
- 5 New mode-matching method
 - Mode-matching basics
 - Closed-form integrals of Helmholtz modes
 - Closed-form integrals of radial Pridmore-Brown modes
 - Mode-matching based on closed form integrals of PB modes
 - Numerical results: comparing CMM and BLM
- 6 Conclusions
 - Epilogue

Slowly varying modes:

Assumptions

- $Z(x)$ has an inherent length scale $L \gg d$, no sudden changes.

We rewrite

$$Z := Z(\varepsilon x) = Z(X), \quad \varepsilon = \frac{d}{L} \ll 1. \quad X = \varepsilon x.$$

- No modal interaction (reflection, cut-on/cut-off, etc)
- Mode, slowly varying in axial direction (WKB Ansatz)

$$\tilde{p}_m(r, X) = P(r, X) \exp \left(\frac{i}{\varepsilon} \int_0^X \kappa(\eta) d\eta \right)$$

Eigenfunction $P(r, X)$ and wave number $\kappa(X)$ to be found.

- Expand in ε

$$P(r, X) = P_0(r, X) + \varepsilon P_1(r, X) + O(\varepsilon^2)$$

- To leading order, the slowly varying mode of order m, μ

$$P_0(r, X) = N(X)\psi_{m\mu}(r, X), \quad \text{with} \quad \kappa = \kappa_{m\mu}(X)$$

where $\psi_{m\mu}(r, X)$ and $\kappa_{m\mu}(X)$ are modal solutions per X

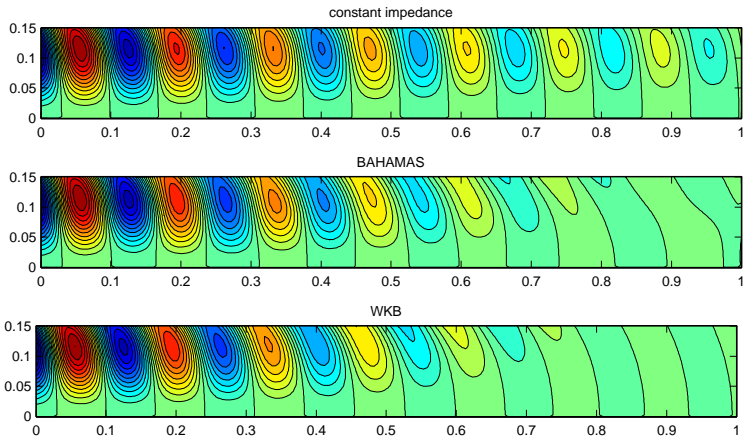
- $N(X)$ is found from solvability condition for P_1 , eventually leading to

$$N(X)^2 = N_0^2 \exp \left(- \int_0^X \frac{f(\eta)}{g(\eta)} d\eta \right)$$

where $f(X), g(X)$ are complicated but explicit functions of $X, \omega, u_0, \rho_0, c_0, Z(X), \psi_{m\mu}$, and $\kappa_{m\mu}$.

Numerical results: linear $Z(X)$

Linear $Z(X)$



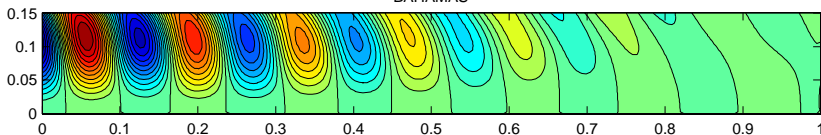
$Z/\rho_{\infty}c_{\infty}$ varies linearly from $1.5 - i$ to $1.5 + i$. BAHAMAS: 10 segments.

\Rightarrow x -dependency of Z is important

\Rightarrow BAHAMAS and WKB agree well ($\varepsilon \approx 0.2$)

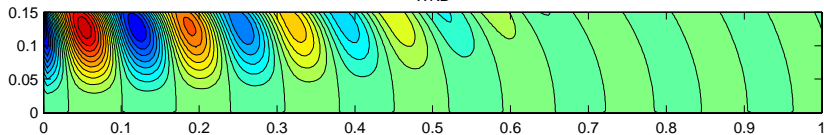
Non-uniform velocity

BAHAMAS



(a) Uniform mean flow velocity with $u_0/c_\infty = 0.3$.

WKB



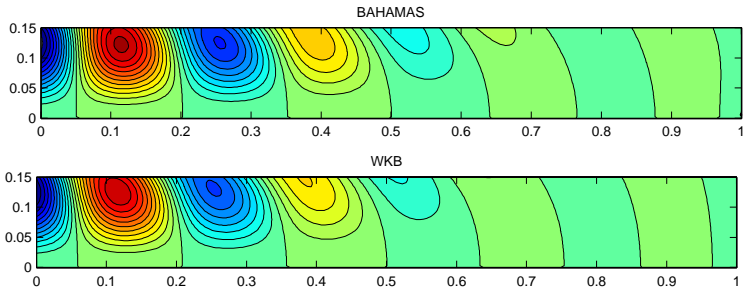
(b) $u_0/c_\infty = 0.3 \cdot \frac{4}{3}(1 - \frac{1}{2}r^2)$

$\omega d/c_\infty = 10$, $m = 2$, $\mu = 1$, $Z/\rho_\infty c_\infty$ varies linearly from $1.5 - i$ to $1.5 + i$
so $\varepsilon \approx 0.2$.

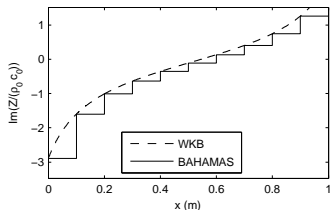
\Rightarrow Non-uniformity of mean flow velocity is important

Numerical results: Helmholtz resonator (no resonance)

Helmholtz resonator (no resonance)



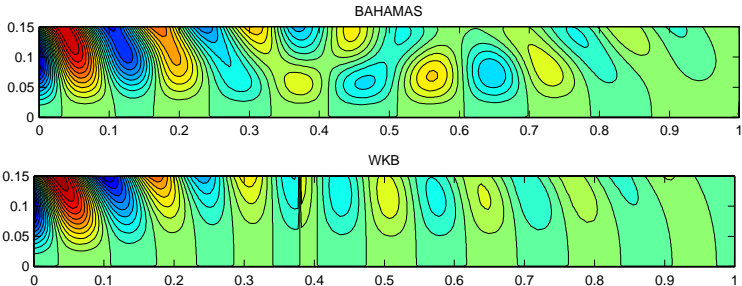
$\omega d/c_\infty = 6$, $m = 2$, $\mu = 1$, uniform mean flow velocity $u_0/c_\infty = 0.3$



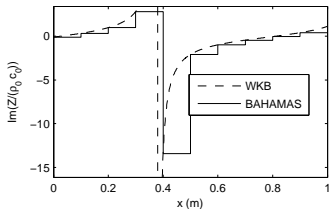
\Rightarrow No resonance and $\varepsilon \approx 0.3$: BAHAMAS and WKB show good agreement

Numerical results: Helmholtz resonator (passing resonance)

Helmholtz resonator (passing resonance)

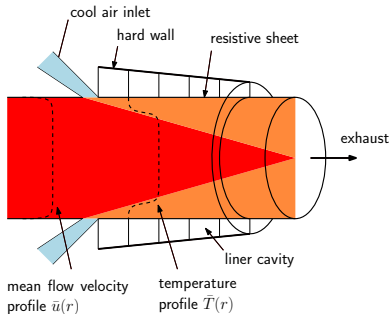


$\omega d/c_\infty = 10$, $m = 2$, $\mu = 1$, uniform mean flow velocity $u_0/c_\infty = 0.3$.

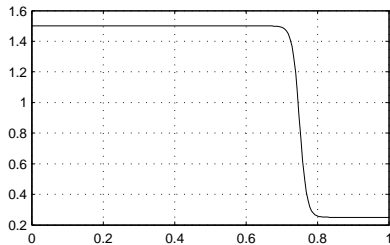


\Rightarrow Resonance: WKB assumptions not valid ($Z(x)$ not slowly varying, intermodal scattering)

Realistic APU exhaust: strong temperature gradient



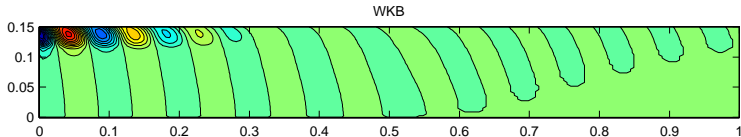
(a) APU exhaust duct geometry with cool air inlet.



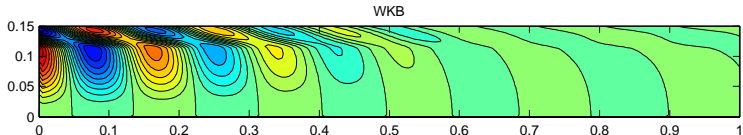
(b) Temperature profile

$$T/T_\infty = \frac{1}{4} + \frac{5}{8} \left(1 + \tanh \left(50 \left(\frac{3}{4} - r \right) \right) \right).$$

Numerical results: strong temperature gradient



(a) WKB, $\mu = 1$.



(b) WKB, $\mu = 2$.

$$\omega d/c_\infty = 10, m = 2, \text{ uniform velocity } u_0/c_\infty = 0.3, \\ Z(x)/\rho_\infty c_\infty \text{ linear: } 1.5 - i \text{ to } 1.5 + i.$$

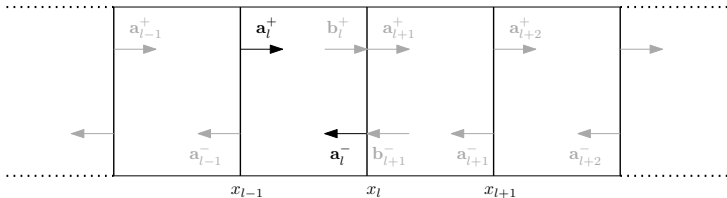
\Rightarrow 2 different sound speeds: 2 *concentric ducts*

Sound refracts from warm to cold

Enhances effect of lining

- 1 Background & motivation
- 2 Pridmore-Brown modes
 - Model & equations
 - Numerical method: COLNEW and path-following
- 3 Options for varying Z
- 4 WKB for slowly varying Z
- 5 New mode-matching method**
 - Mode-matching basics
 - Closed-form integrals of Helmholtz modes
 - Closed-form integrals of radial Pridmore-Brown modes
 - Mode-matching based on closed form integrals of PB modes
 - Numerical results: comparing CMM and BLM
- 6 Conclusions
 - Epilogue

Mode-Matching Basics

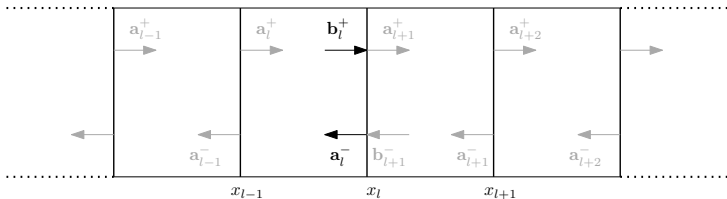


Total field in segment l : sum of left- and right-running waves

$$p_l(x, r) = \sum_{\mu=1}^{\infty} \left(a_{l,\mu}^+ P_{l,\mu}^+(r) e^{ik_{l,\mu}^+(x-x_{l-1})} + a_{l,\mu}^- P_{l,\mu}^-(r) e^{ik_{l,\mu}^-(x-x_l)} \right)$$

(same for velocity)

Mode-Matching Basics

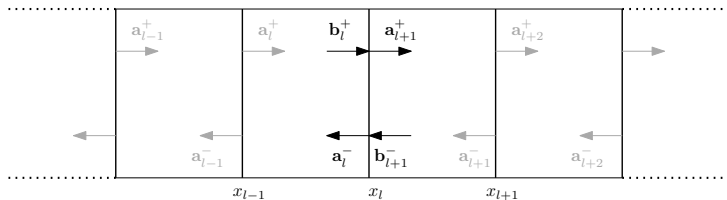


At the interface at $x = x_l$:

$$p_l(r) = \sum_{\mu=1}^{\mu^{\max}} \left(b_{l,\mu}^+ P_{l,\mu}^+(r) + a_{l,\mu}^- P_{l,\mu}^-(r) \right).$$

(same for velocity)

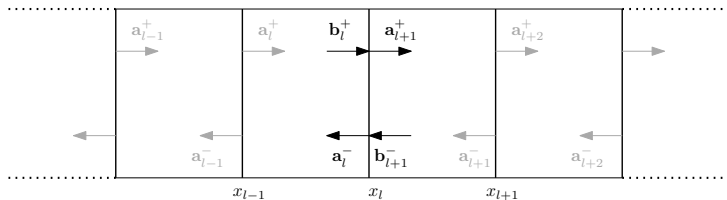
Mode-Matching Basics



Continuity of pressure at $x = x_l$ leads to

$$p_l(x_l, r) = p_{l+1}(x_l, r)$$

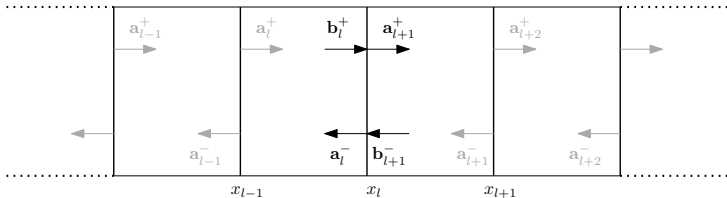
Mode-Matching Basics



Continuity of pressure at $x = x_l$ leads to

$$\sum_{\mu=1}^{\mu^{\max}} \left(b_{l,\mu}^+ P_{l,\mu}^+ + a_{l,\mu}^- P_{l,\mu}^- \right) = \sum_{\mu=1}^{\mu^{\max}} \left(a_{l+1,\mu}^+ P_{l+1,\mu}^+ + b_{l+1,\mu}^- P_{l+1,\mu}^- \right)$$

Mode-Matching Basics

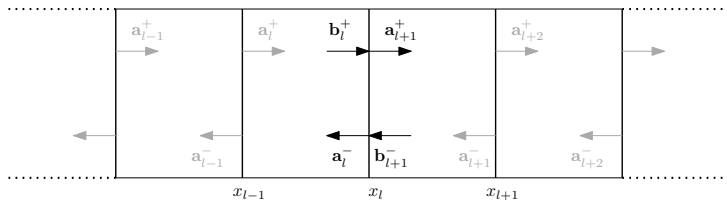


inner products with suitable test functions Ψ_ν , e.g. $= J_m(\alpha_\nu r)$

$$\sum_{\mu=1}^{\mu^{\max}} \left(b_{l,\mu}^+ (P_{l,\mu}^+, \Psi_\nu) + a_{l,\mu}^- (P_{l,\mu}^-, \Psi_\nu) \right)$$

$$= \sum_{\mu=1}^{\mu^{\max}} \left(a_{l+1,\mu}^+ (P_{l+1,\mu}^+, \Psi_\nu) + b_{l+1,\mu}^- (P_{l+1,\mu}^-, \Psi_\nu) \right)$$

Mode-Matching Basics

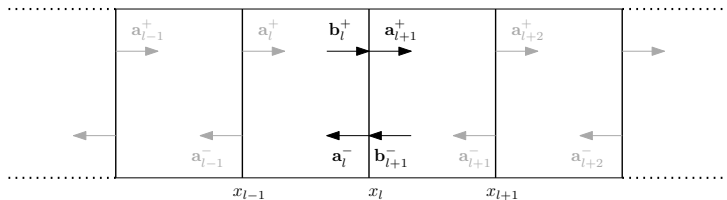


inner products with suitable test functions Ψ_ν , e.g. $= J_m(\alpha_\nu r)$

$$\begin{aligned} \sum_{\mu=1}^{\mu^{\max}} \left(b_{l,\mu}^+(P_{l,\mu}^+, \Psi_\nu) + a_{l,\mu}^-(P_{l,\mu}^-, \Psi_\nu) \right) \\ = \sum_{\mu=1}^{\mu^{\max}} \left(a_{l+1,\mu}^+(P_{l+1,\mu}^+, \Psi_\nu) + b_{l+1,\mu}^-(P_{l+1,\mu}^-, \Psi_\nu) \right) \end{aligned}$$

Similar for continuity of axial velocity.

Mode-Matching Basics



Results in linear system to be solved

$$\begin{bmatrix} \mathbf{A}^+ & \mathbf{A}^- \\ \mathbf{C}^+ & \mathbf{C}^- \end{bmatrix} \begin{bmatrix} \mathbf{b}_l^+ \\ \mathbf{a}_l^- \end{bmatrix} = \begin{bmatrix} \mathbf{B}^+ & \mathbf{B}^- \\ \mathbf{D}^+ & \mathbf{D}^- \end{bmatrix} \begin{bmatrix} \mathbf{a}_{l+1}^+ \\ \mathbf{b}_{l+1}^- \end{bmatrix}.$$

Computing inner products

Matrix entries are inner products

$$A_{\nu\mu}^{\pm} = (P_{l,\mu}^{\pm}, \Psi_{\nu}) = \int_0^d P_{l,\mu}^{\pm}(r) \Psi_{\nu}(r) r \, dr$$

Computing inner products

Matrix entries are inner products

$$A_{\nu\mu}^{\pm} = (P_{l,\mu}^{\pm}, \Psi_{\nu}) = \int_0^d P_{l,\mu}^{\pm}(r) \Psi_{\nu}(r) r \, dr$$

Note that for non-uniform flow:

- $P_{l,\mu}^{\pm}$ is determined numerically
- **All** inner-products have to be determined at **all** interfaces by quadrature
- $P_{l,\mu}^{\pm}$ and Ψ_{ν} are oscillatory \Rightarrow numerical problems

Computing inner products

Matrix entries are inner products

$$A_{\nu\mu}^{\pm} = (P_{l,\mu}^{\pm}, \Psi_{\nu}) = \int_0^d P_{l,\mu}^{\pm}(r) \Psi_{\nu}(r) r \, dr$$

Note that for non-uniform flow:

- $P_{l,\mu}^{\pm}$ is determined numerically
- **All** inner-products have to be determined at **all** interfaces by quadrature
- $P_{l,\mu}^{\pm}$ and Ψ_{ν} are oscillatory \Rightarrow numerical problems

Problem

Computing inner products numerically is expensive / less accurate

Computing inner products

Matrix entries are inner products

$$A_{\nu\mu}^{\pm} = (P_{l,\mu}^{\pm}, \Psi_{\nu}) = \int_0^d P_{l,\mu}^{\pm}(r) \Psi_{\nu}(r) r \, dr$$

Note that for non-uniform flow:

- $P_{l,\mu}^{\pm}$ is determined numerically
- **All** inner-products have to be determined at **all** interfaces by quadrature
- $P_{l,\mu}^{\pm}$ and Ψ_{ν} are oscillatory \Rightarrow numerical problems

Problem

Computing inner products numerically is expensive / less accurate

€1.000.000 question

Can we find closed-form expressions for the inner-product?

Computing inner products

Matrix entries are inner products

$$A_{\nu\mu}^{\pm} = (P_{l,\mu}^{\pm}, \Psi_{\nu}) = \int_0^d P_{l,\mu}^{\pm}(r) \Psi_{\nu}(r) r \, dr$$

Note that for non-uniform flow:

- $P_{l,\mu}^{\pm}$ is determined numerically
- **All** inner-products have to be determined at **all** interfaces by quadrature
- $P_{l,\mu}^{\pm}$ and Ψ_{ν} are oscillatory \Rightarrow numerical problems

Problem

Computing inner products numerically is expensive / less accurate

€1.000.000 question

Can we find closed-form expressions for the inner-product? No

Computing inner products

Matrix entries are inner products

$$A_{\nu\mu}^{\pm} = (P_{l,\mu}^{\pm}, \Psi_{\nu}) = \int_0^d P_{l,\mu}^{\pm}(r) \Psi_{\nu}(r) r \, dr$$

Note that for non-uniform flow:

- $P_{l,\mu}^{\pm}$ is determined numerically
- **All** inner-products have to be determined at **all** interfaces by quadrature
- $P_{l,\mu}^{\pm}$ and Ψ_{ν} are oscillatory \Rightarrow numerical problems

Problem

Computing inner products numerically is expensive / less accurate

€1.000.000 question

Can we find closed-form expressions for *other* 'inner-product'?

Computing inner products

Matrix entries are inner products

$$A_{\nu\mu}^{\pm} = (P_{l,\mu}^{\pm}, \Psi_{\nu}) = \int_0^d P_{l,\mu}^{\pm}(r) \Psi_{\nu}(r) r \, dr$$

Note that for non-uniform flow:

- $P_{l,\mu}^{\pm}$ is determined numerically
- **All** inner-products have to be determined at **all** interfaces by quadrature
- $P_{l,\mu}^{\pm}$ and Ψ_{ν} are oscillatory \Rightarrow numerical problems

Problem

Computing inner products numerically is expensive / less accurate

€1.000.000 question

Can we find closed-form expressions for *other* 'inner-product'? Yes!

From Classical to a New Mode-matching method

Summary of new matching method

Classical \rightarrow **new** mode-matching

$$(P_\mu, \Psi_\nu) \rightarrow \langle \mathbf{F}_\mu, \mathbf{\Psi}_\nu \rangle$$

From Classical to a New Mode-matching method

Summary of new matching method

Classical (CMM) \rightarrow **new (BLM)** mode-matching

$$(P_\mu, \Psi_\nu) \rightarrow \langle \mathbf{F}_\mu, \boldsymbol{\Psi}_\nu \rangle$$

with $\Psi_\nu = J_m(\alpha_\nu r)$

with $\boldsymbol{\Psi}_\nu = \mathbf{F}_\nu$, $\mathbf{F} = [P, U, V, W]$

From Classical to a New Mode-matching method

Summary of new matching method

Classical (CMM) \rightarrow **new (BLM)** mode-matching

$$(P_\mu, \Psi_\nu) \quad \rightarrow \quad \langle \mathbf{F}_\mu, \boldsymbol{\Psi}_\nu \rangle$$

$$= \int_0^d P_\mu \Psi_\nu r \, dr \quad \rightarrow \quad = \int_0^d \left[w_1 P_\mu P_\nu + w_2 U_\mu P_\nu + w_3 (V_\mu V_\nu + W_\mu W_\nu) \right] r \, dr$$

$$\text{with } \Psi_\nu = J_m(\alpha_\nu r)$$

$$\text{with } \boldsymbol{\Psi}_\nu = \mathbf{F}_\nu, \quad \mathbf{F} = [P, U, V, W]$$

From Classical to a New Mode-matching method

Summary of new matching method

Classical (CMM) \rightarrow **new (BLM)** mode-matching

$$(P_\mu, \Psi_\nu) \rightarrow \langle \mathbf{F}_\mu, \boldsymbol{\Psi}_\nu \rangle$$

$$= \int_0^d P_\mu \Psi_\nu r \, dr \rightarrow = \int_0^d [w_1 P_\mu P_\nu + w_2 U_\mu P_\nu + w_3 (V_\mu V_\nu + W_\mu W_\nu)] r \, dr$$

$$\text{quadrature} \rightarrow = \frac{id}{k_\mu - k_\nu} \left[\frac{P_\nu V_\mu - V_\nu P_\mu}{\Omega_\nu} \right]_{r=d}$$

$$\text{with } \Psi_\nu = J_m(\alpha_\nu r)$$

$$\text{with } \boldsymbol{\Psi}_\nu = \mathbf{F}_\nu, \quad \mathbf{F} = [P, U, V, W]$$

From Classical to a New Mode-matching method

Summary of new matching method

Classical (CMM) \rightarrow **new (BLM)** mode-matching

$$(P_\mu, \Psi_\nu) \quad \rightarrow \quad \langle \mathbf{F}_\mu, \boldsymbol{\Psi}_\nu \rangle$$

$$= \int_0^d P_\mu \Psi_\nu r \, dr \quad \rightarrow \quad = \int_0^d \left[w_1 P_\mu P_\nu + w_2 U_\mu P_\nu \right. \\ \left. + w_3 (V_\mu V_\nu + W_\mu W_\nu) \right] r \, dr$$

$$\text{quadrature} \quad \rightarrow \quad = \frac{\text{id}}{k_\mu - k_\nu} \left[\frac{P_\nu V_\mu - V_\nu P_\mu}{\Omega_\nu} \right]_{r=d}$$

$$\text{with } \Psi_\nu = J_m(\alpha_\nu r)$$

$$\text{with } \boldsymbol{\Psi}_\nu = \mathbf{F}_\nu, \quad \mathbf{F} = [P, U, V, W]$$

expensive
less accurate

\rightarrow

cheap
accurate

Closed form integrals of 2D eigenmodes

Prototype example of *Generalised Prid-Brown* : Helmholtz eqn

$$\nabla^2 \psi + \beta^2 \psi = 0$$

on arbitrarily shaped cross-section \mathcal{A}

Closed form integrals of 2D eigenmodes

Prototype example of *Generalised Prid-Brown* : Helmholtz eqn

$$\nabla^2 \psi + \beta^2 \psi = 0$$

$$\nabla^2 \phi + \alpha^2 \phi = 0$$

on arbitrarily shaped cross-section \mathcal{A}

Closed form integrals of 2D eigenmodes

Prototype example of *Generalised Prid-Brown* : Helmholtz eqn

$$\phi (\nabla^2 \psi + \beta^2 \psi) = 0$$

$$\psi (\nabla^2 \phi + \alpha^2 \phi) = 0$$

on arbitrarily shaped cross-section \mathcal{A}

Closed form integrals of 2D eigenmodes

Prototype example of *Generalised Prid-Brown* : Helmholtz eqn

$$\phi (\nabla^2 \psi + \beta^2 \psi) = 0$$

$$\psi (\nabla^2 \phi + \alpha^2 \phi) = 0$$

on arbitrarily shaped cross-section \mathcal{A}

Subtract

$$(\alpha^2 - \beta^2) \phi \psi = \phi \nabla^2 \psi - \psi \nabla^2 \phi$$

Closed form integrals of 2D eigenmodes

Prototype example of *Generalised Prid-Brown* : Helmholtz eqn

$$\phi (\nabla^2 \psi + \beta^2 \psi) = 0$$

$$\psi (\nabla^2 \phi + \alpha^2 \phi) = 0$$

on arbitrarily shaped cross-section \mathcal{A}

Subtract and integrate over \mathcal{A}

$$(\alpha^2 - \beta^2) \iint_{\mathcal{A}} \phi \psi \, dS = \iint_{\mathcal{A}} (\phi \nabla^2 \psi - \psi \nabla^2 \phi) \, dS$$

Closed form integrals of 2D eigenmodes

Prototype example of *Generalised Prid-Brown* : Helmholtz eqn

$$\phi (\nabla^2 \psi + \beta^2 \psi) = 0$$

$$\psi (\nabla^2 \phi + \alpha^2 \phi) = 0$$

on arbitrarily shaped cross-section \mathcal{A}

Subtract and integrate over \mathcal{A}

$$(\alpha^2 - \beta^2) \iint_{\mathcal{A}} \phi \psi \, dS = \iint_{\mathcal{A}} \nabla \cdot (\phi \nabla \psi - \psi \nabla \phi) \, dS$$

Closed form integrals of 2D eigenmodes

Prototype example of *Generalised Prid-Brown* : Helmholtz eqn

$$\phi (\nabla^2 \psi + \beta^2 \psi) = 0$$

$$\psi (\nabla^2 \phi + \alpha^2 \phi) = 0$$

on arbitrarily shaped cross-section \mathcal{A}

Subtract and integrate over \mathcal{A}

$$(\alpha^2 - \beta^2) \iint_{\mathcal{A}} \phi \psi \, dS = \iint_{\mathcal{A}} \overset{\text{GAUSS}}{\downarrow} \nabla \cdot (\phi \nabla \psi - \psi \nabla \phi) \, dS$$

Closed form integrals of 2D eigenmodes

Prototype example of *Generalised Prid-Brown* : Helmholtz eqn

$$\phi (\nabla^2 \psi + \beta^2 \psi) = 0$$

$$\psi (\nabla^2 \phi + \alpha^2 \phi) = 0$$

on arbitrarily shaped cross-section \mathcal{A}

Subtract and integrate over \mathcal{A}

$$(\alpha^2 - \beta^2) \iint_{\mathcal{A}} \phi \psi \, dS = \int_{\Gamma} (\overset{\text{GAUSS}}{\downarrow} \phi \nabla \psi \cdot \mathbf{n} - \psi \nabla \phi \cdot \mathbf{n}) \, d\ell$$

Closed form integrals of 2D eigenmodes

Prototype example of *Generalised Prid-Brown* : Helmholtz eqn

$$\phi (\nabla^2 \psi + \beta^2 \psi) = 0$$

$$\psi (\nabla^2 \phi + \alpha^2 \phi) = 0$$

on arbitrarily shaped cross-section \mathcal{A}

Subtract and integrate over \mathcal{A}

$$(\alpha^2 - \beta^2) \iint_{\mathcal{A}} \phi \psi \, dS = \int_{\Gamma} (\phi \nabla \psi \cdot \mathbf{n} - \psi \nabla \phi \cdot \mathbf{n}) \, d\ell$$

2D inner-product for Helmholtz eigenfunctions

$$\langle\langle \phi, \psi \rangle\rangle = \frac{1}{\alpha^2 - \beta^2} \int_{\Gamma} (\phi \nabla \psi \cdot \mathbf{n} - \psi \nabla \phi \cdot \mathbf{n}) \, d\ell,$$

for arbitrary boundary conditions on ϕ and ψ

What if $\alpha = \beta$ and $\phi = \psi$? Something similar.

Closed form integrals of 1D eigenmodes

- Circular duct: Helmholtz equation \rightarrow Bessel equation
- Substitute into 2D inner-product:

$$\phi = J_m(\alpha r) e^{im\theta}, \psi = J_m(\beta r) e^{-im\theta}$$

Closed form integrals of 1D eigenmodes

- Circular duct: Helmholtz equation \rightarrow Bessel equation
- Substitute into 2D inner-product:

$$\phi = J_m(\alpha r) e^{im\theta}, \psi = J_m(\beta r) e^{-im\theta}$$

1D inner-product of Bessel functions

$$\begin{aligned}\langle J_m(\alpha r), J_m(\beta r) \rangle &= \int_0^1 J_m(\alpha r) J_m(\beta r) r dr \\ &= \frac{1}{\alpha^2 - \beta^2} [\beta J_m(\alpha) J'_m(\beta) - \alpha J'_m(\alpha) J_m(\beta)]\end{aligned}$$

Closed form integrals of 1D eigenmodes

- Circular duct: Helmholtz equation \rightarrow Bessel equation
- Substitute into 2D inner-product:

$$\phi = J_m(\alpha r) e^{im\theta}, \psi = J_m(\beta r) e^{-im\theta}$$

1D inner-product of Bessel functions

$$\begin{aligned}\langle J_m(\alpha r), J_m(\beta r) \rangle &= \int_0^1 J_m(\alpha r) J_m(\beta r) r dr \\ &= \frac{1}{\alpha^2 - \beta^2} [\beta J_m(\alpha) J'_m(\beta) - \alpha J'_m(\alpha) J_m(\beta)]\end{aligned}$$

If $\alpha = \beta$: something similar.

By analogous manipulations . . .

By analogous manipulations . . .

- Define vector of shape functions $\mathbf{F}(y, z) = [P, U, V, W]$
- P solution of Generalised PB equation, U, V, W follow from P

By analogous manipulations ...

- Define vector of shape functions $\mathbf{F}(y, z) = [P, U, V, W]$
- P solution of Generalised PB equation, U, V, W follow from P

Similarly to 2D Helmholtz example, it can be found:

Closed form integral of parallel flow modes

$$\begin{aligned}\langle\langle \mathbf{F}, \tilde{\mathbf{F}} \rangle\rangle &= \\ \iint_{\mathcal{A}} \frac{1}{\tilde{\Omega}} &\left[\left(\frac{u_0}{\rho_0 c_0^2} + \frac{\tilde{k}}{\rho_0 \tilde{\Omega}} \right) \tilde{P}P + \frac{\omega}{\tilde{\Omega}} \tilde{P}U - \rho_0 u_0 (\tilde{V}V + \tilde{W}W) \right] dS \\ &= \frac{i}{k - \tilde{k}} \int_{\Gamma} \frac{\tilde{P}(Vn_y + Wn_z) - (\tilde{V}n_y + \tilde{W}n_z)P}{\tilde{\Omega}} d\ell,\end{aligned}$$

By analogous manipulations ...

- Define vector of shape functions $\mathbf{F}(y, z) = [P, U, V, W]$
- P solution of Generalised PB equation, U, V, W follow from P

Similarly to 2D Helmholtz example, it can be found:

Closed form integral of parallel flow modes

$$\begin{aligned}\langle\langle \mathbf{F}, \tilde{\mathbf{F}} \rangle\rangle &= \\ \iint_{\mathcal{A}} \frac{1}{\tilde{\Omega}} \left[\left(\frac{u_0}{\rho_0 c_0^2} + \frac{\tilde{k}}{\rho_0 \tilde{\Omega}} \right) \tilde{P} P + \frac{\omega}{\tilde{\Omega}} \tilde{P} U - \rho_0 u_0 (\tilde{V} V + \tilde{W} W) \right] dS \\ &= \frac{i}{k - \tilde{k}} \int_{\Gamma} \frac{\tilde{P} (V n_y + W n_z) - (\tilde{V} n_y + \tilde{W} n_z) P}{\tilde{\Omega}} d\ell,\end{aligned}$$

Something similar for $k = \tilde{k}$.

Closed form integrals for radial Pridmore-Brown modes

Substitute for circular symmetric geometry...

Substitute for circular symmetric geometry...

modes of the form $\mathbf{F}(r) e^{\pm im\theta}$

$$\mathbf{F}(r) = [P(r), U(r), V(r), W(r)]$$

Substitute for circular symmetric geometry...

modes of the form $\mathbf{F}(r) e^{\pm im\theta}$

$$\mathbf{F}(r) = [P(r), U(r), V(r), W(r)]$$

- P solution of the radial Pridmore-Brown equation
- U, V, W follow from P

Closed form integrals for radial Pridmore-Brown modes

Substitute for circular symmetric geometry...

modes of the form $\mathbf{F}(r) e^{\pm im\theta}$

$$\mathbf{F}(r) = [P(r), U(r), V(r), W(r)]$$

- P solution of the radial Pridmore-Brown equation
- U, V, W follow from P

Exact integrals of radial Pridmore-Brown modes

$$\begin{aligned}\langle \mathbf{F}, \tilde{\mathbf{F}} \rangle &= \\ \int_0^d \frac{1}{\tilde{\Omega}} \left[\left(\frac{u_0}{\rho_0 c_0^2} + \frac{\tilde{k}}{\rho_0 \tilde{\Omega}} \right) P \tilde{P} + \frac{\omega}{\tilde{\Omega}} U \tilde{P} - \rho_0 u_0 (V \tilde{V} + W \tilde{W}) \right] r \, dr \\ &= \frac{id}{k - \tilde{k}} \left[\frac{\tilde{P}V - \tilde{V}P}{\tilde{\Omega}} \right]_{r=d}\end{aligned}$$

Weighted products of Pridmore-Brown eigenfunctions.

Something similar for $k = \tilde{k}$.

Some special cases

With Ingard-Myers condition (slipping flow)

$$\langle \mathbf{F}, \tilde{\mathbf{F}} \rangle = \left[\frac{\text{id} \tilde{P} P}{(k - \tilde{k}) \tilde{\Omega} \omega} \left(\frac{\Omega}{Z} - \frac{\tilde{\Omega}}{\tilde{Z}} \right) \right]_{r=d}$$

Some special cases

With Ingard-Myers condition (slipping flow)

$$\langle \mathbf{F}, \tilde{\mathbf{F}} \rangle = \left[\frac{\text{id} \tilde{P} P}{(k - \tilde{k}) \tilde{\Omega} \omega} \left(\frac{\Omega}{Z} - \frac{\tilde{\Omega}}{\tilde{Z}} \right) \right]_{r=d}$$

For hard walls:

$$\text{"orthogonal":} \quad \begin{cases} \langle \mathbf{F}, \tilde{\mathbf{F}} \rangle = 0 \\ \langle \mathbf{F}, \mathbf{F} \rangle \neq 0 \end{cases}$$

Some special cases

With Ingard-Myers condition (slipping flow)

$$\langle \mathbf{F}, \tilde{\mathbf{F}} \rangle = \left[\frac{\text{id} \tilde{P} P}{(k - \tilde{k}) \tilde{\Omega} \omega} \left(\frac{\Omega}{Z} - \frac{\tilde{\Omega}}{\tilde{Z}} \right) \right]_{r=d}$$

For hard walls:

$$\text{“orthogonal”}: \quad \begin{cases} \langle \mathbf{F}, \tilde{\mathbf{F}} \rangle = 0 \\ \langle \mathbf{F}, \mathbf{F} \rangle \neq 0 \end{cases}$$

In case of no-slip flow, $u_0(d) = 0$:

$$\langle \mathbf{F}, \tilde{\mathbf{F}} \rangle = \left[\frac{\text{id} \tilde{P} P}{(k - \tilde{k}) \omega} \left(\frac{1}{Z} - \frac{1}{\tilde{Z}} \right) \right]_{r=d}$$

Some special cases

With Ingard-Myers condition (slipping flow)

$$\langle \mathbf{F}, \tilde{\mathbf{F}} \rangle = \left[\frac{\text{id}\tilde{P}P}{(k - \tilde{k})\tilde{\Omega}\omega} \left(\frac{\Omega}{Z} - \frac{\tilde{\Omega}}{\tilde{Z}} \right) \right]_{r=d}$$

For hard walls:

$$\text{“orthogonal”}: \quad \begin{cases} \langle \mathbf{F}, \tilde{\mathbf{F}} \rangle = 0 \\ \langle \mathbf{F}, \mathbf{F} \rangle \neq 0 \end{cases}$$

In case of no-slip flow, $u_0(d) = 0$:

$$\langle \mathbf{F}, \tilde{\mathbf{F}} \rangle = \left[\frac{\text{id}\tilde{P}P}{(k - \tilde{k})\omega} \left(\frac{1}{Z} - \frac{1}{\tilde{Z}} \right) \right]_{r=d}$$

For hard walls, or same impedance $Z = \tilde{Z}$:

$$\text{“orthogonal”}: \quad \begin{cases} \langle \mathbf{F}, \tilde{\mathbf{F}} \rangle = 0 \\ \langle \mathbf{F}, \mathbf{F} \rangle \neq 0 \end{cases}$$

Classic mode-matching (CMM)

$$\begin{aligned} \sum_{\mu=1}^{\mu_l} b_{l,\mu}^+(P_{l,\mu}^+, \Psi_\nu) + a_{l,\mu}^-(P_{l,\mu}^-, \Psi_\nu) \\ = \sum_{\mu=1}^{\mu_{l+1}} a_{l+1,\mu}^+(P_{l+1,\mu}^+, \Psi_\nu) + b_{l+1,\mu}^-(P_{l+1,\mu}^-, \Psi_\nu) \end{aligned}$$

(same for velocity) with test functions (for example)

$$\Psi_\nu = J_m(\alpha_\nu r)$$

Classic mode-matching (CMM)

$$\begin{aligned} \sum_{\mu=1}^{\mu_l} b_{l,\mu}^+(P_{l,\mu}^+, \Psi_\nu) + a_{l,\mu}^-(P_{l,\mu}^-, \Psi_\nu) \\ = \sum_{\mu=1}^{\mu_{l+1}} a_{l+1,\mu}^+(P_{l+1,\mu}^+, \Psi_\nu) + b_{l+1,\mu}^-(P_{l+1,\mu}^-, \Psi_\nu) \end{aligned}$$

(same for velocity) with test functions (for example)

$$\Psi_\nu = J_m(\alpha_\nu r)$$

Quadrature required for (P_μ, Ψ_ν) terms (non-uniform flow)

Bilinear map-based (BLM) mode-matching

$$\begin{aligned} \sum_{\mu=1}^{\mu_l} b_{l,\mu}^+ \langle \mathbf{F}_{l,\mu}^+, \boldsymbol{\Psi}_\nu \rangle + a_{l,\mu}^- \langle \mathbf{F}_{l,\mu}^-, \boldsymbol{\Psi}_\nu \rangle \\ = \sum_{\mu=1}^{\mu_{l+1}} a_{l+1,\mu}^+ \langle \mathbf{F}_{l+1,\mu}^+, \boldsymbol{\Psi}_\nu \rangle + b_{l+1,\mu}^- \langle \mathbf{F}_{l+1,\mu}^-, \boldsymbol{\Psi}_\nu \rangle \end{aligned}$$

but now as test functions the same modes:

$$\boldsymbol{\Psi}_\nu = \mathbf{F}_{l,\nu}$$

Bilinear map-based* (BLM) mode-matching

$$\begin{aligned} \sum_{\mu=1}^{\mu_l} b_{l,\mu}^+ \langle \mathbf{F}_{l,\mu}^+, \boldsymbol{\Psi}_\nu \rangle + a_{l,\mu}^- \langle \mathbf{F}_{l,\mu}^-, \boldsymbol{\Psi}_\nu \rangle \\ = \sum_{\mu=1}^{\mu_{l+1}} a_{l+1,\mu}^+ \langle \mathbf{F}_{l+1,\mu}^+, \boldsymbol{\Psi}_\nu \rangle + b_{l+1,\mu}^- \langle \mathbf{F}_{l+1,\mu}^-, \boldsymbol{\Psi}_\nu \rangle \end{aligned}$$

but now as test functions the same modes:

$$\boldsymbol{\Psi}_\nu = \mathbf{F}_{l,\nu}$$

*Technically not an inner-product, except for no flow or uniform flow.

Bilinear map-based* (BLM) mode-matching

$$\begin{aligned} \sum_{\mu=1}^{\mu_l} b_{l,\mu}^+ \langle \mathbf{F}_{l,\mu}^+, \boldsymbol{\Psi}_\nu \rangle + a_{l,\mu}^- \langle \mathbf{F}_{l,\mu}^-, \boldsymbol{\Psi}_\nu \rangle \\ = \sum_{\mu=1}^{\mu_{l+1}} a_{l+1,\mu}^+ \langle \mathbf{F}_{l+1,\mu}^+, \boldsymbol{\Psi}_\nu \rangle + b_{l+1,\mu}^- \langle \mathbf{F}_{l+1,\mu}^-, \boldsymbol{\Psi}_\nu \rangle \end{aligned}$$

but now as test functions the same modes:

$$\boldsymbol{\Psi}_\nu = \mathbf{F}_{l,\nu}$$

No extra calculations *and* $\langle \mathbf{F}_\mu, \boldsymbol{\Psi}_\nu \rangle$ in closed form

*Technically not an inner-product, except for no flow or uniform flow.

Comparing CMM and BLM

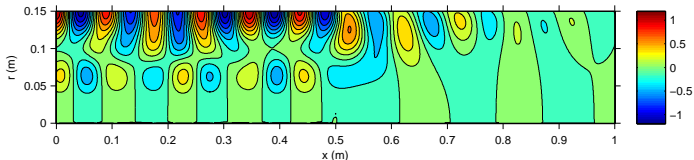
Test configurations

- Length: 1m
- Radius: 15cm
- hard wall – soft wall, interface at $x = 0.5m$
- $\mu^{\max} = 50$ modes in both directions

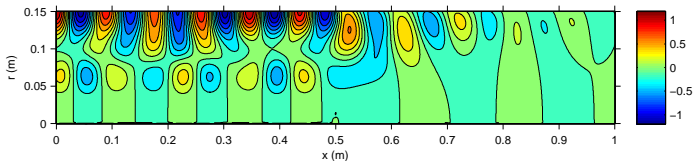
Configuration	I	II	III
Helmholtz & m	$\omega d/c_\infty = 13.86, m = 5$	$\omega d/c_\infty = 8.86, m = 5$	$\omega d/c_\infty = 15, m = 5$
Temperature	$T_0/T_\infty = 1$	$T_0/T_\infty = 1$	$T_0/T_\infty = 2 \log(2)(1 - \frac{r^2}{2})$
Mean flow	$u_0/c_\infty = 0.5 \cdot (1 - r^2)$	$u_0/c_\infty = 0.3 \cdot \frac{4}{3}(1 - \frac{r^2}{2})$	$u_0/c_\infty = 0.3 \cdot \tanh(10(1 - r))$
Impedance	$Z/\rho_\infty c_\infty = 1 - i$	$Z/\rho_\infty c_\infty = 1 + i$	$Z/\rho_\infty c_\infty = 1 - i$
Incident mode	$\mu = 1$	$\mu = 1$	$\mu = 2$

Numerical results — Conf I: no-slip flow, uniform temp

Real part of pressure



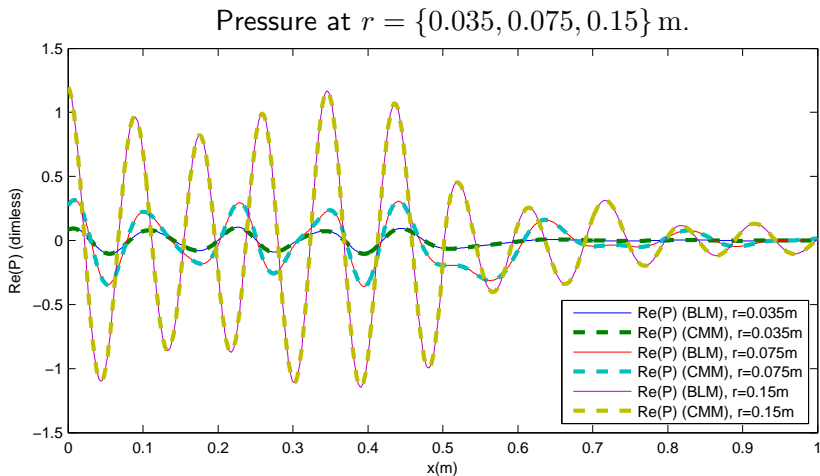
(a) Classical mode-matching.



(b) Bilinear map-based mode-matching.

Perfect match between BLM and CMM results

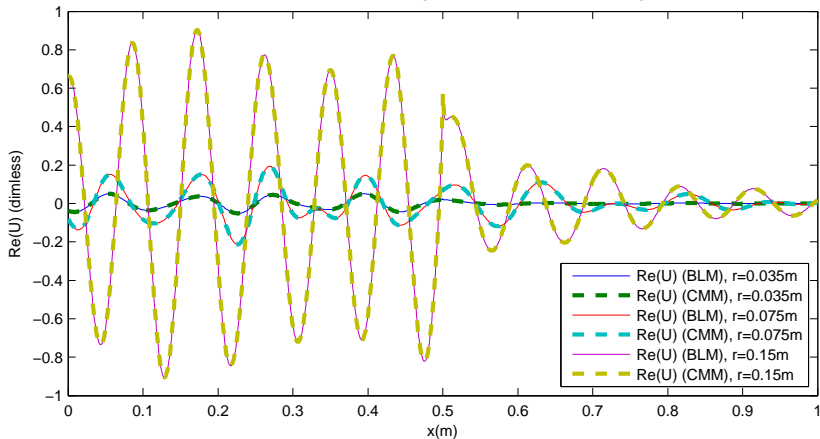
Numerical results — Conf I: no-slip flow, uniform temp



Perfect match between BLM and CMM results

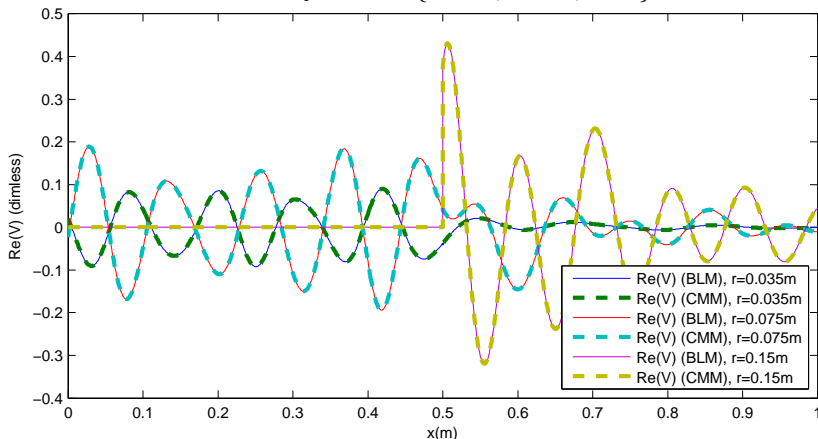
Numerical results — Conf I: no-slip flow, uniform temp

Axial velocity at $r = \{0.035, 0.075, 0.15\}$ m.



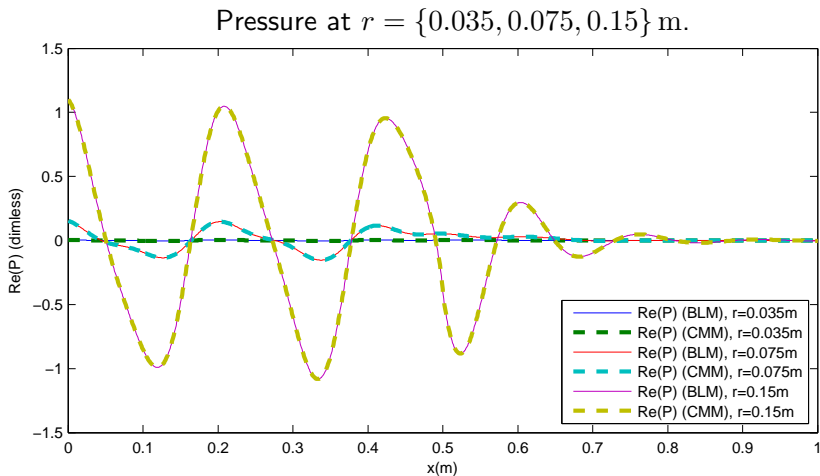
Perfect match between BLM and CMM results

Radial velocity at $r = \{0.035, 0.075, 0.15\}$ m.



Perfect match between BLM and CMM results

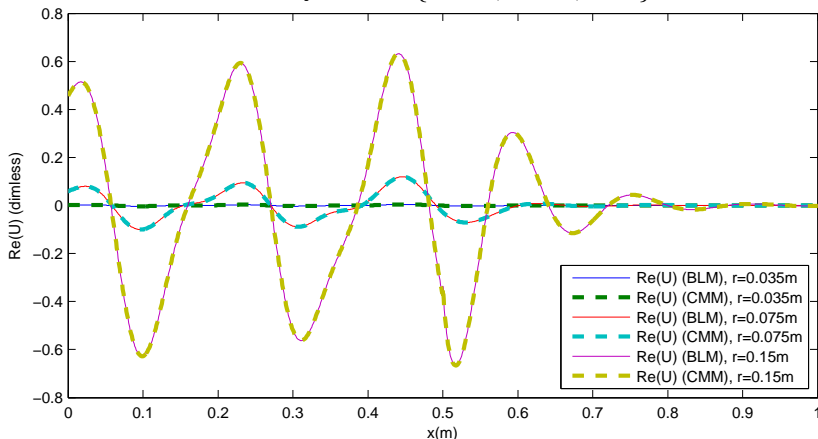
Numerical results — Conf II: slipping flow, uniform temp



Perfect match between BLM and CMM results

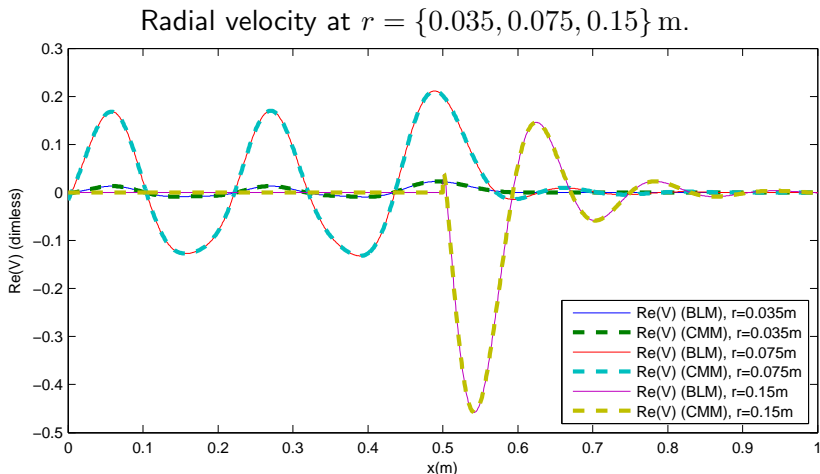
Numerical results — Conf II: slipping flow, uniform temp

Axial velocity at $r = \{0.035, 0.075, 0.15\}$ m.



Perfect match between BLM and CMM results

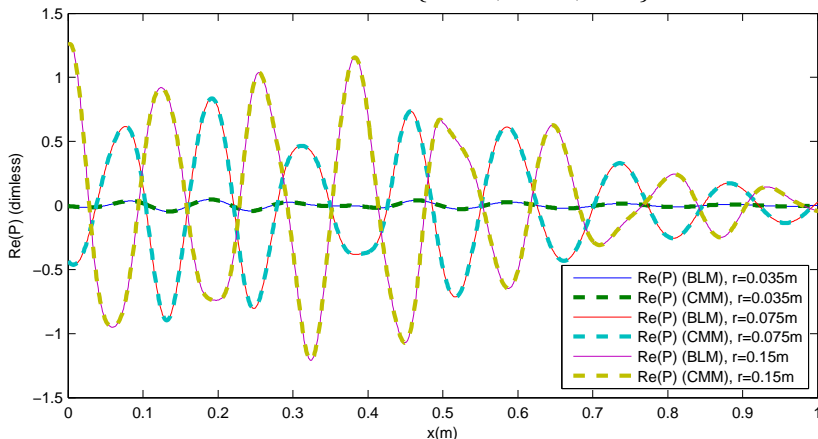
Numerical results — Conf II: slipping flow, uniform temp



Perfect match between BLM and CMM results

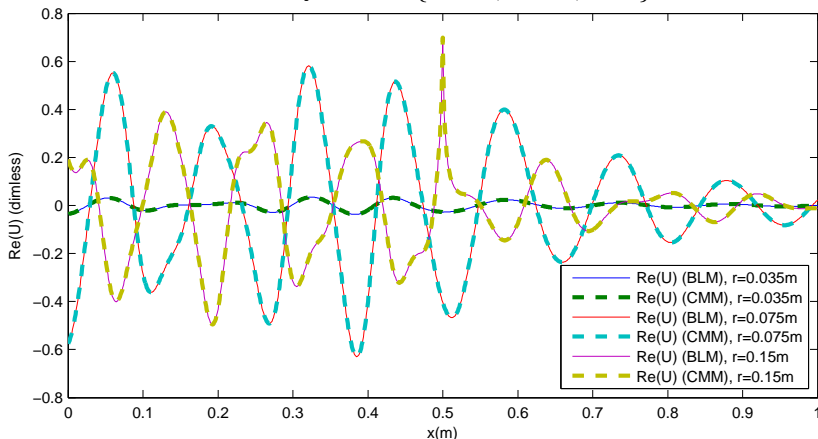
Numerical results — Conf III: bndary layer, non-unif. temp

Pressure at $r = \{0.035, 0.075, 0.15\}$ m.



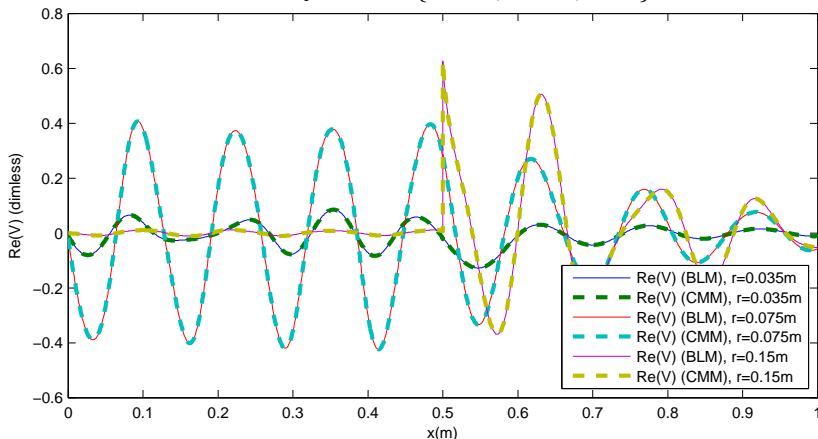
Perfect match between BLM and CMM results

Axial velocity at $r = \{0.035, 0.075, 0.15\}$ m.



Perfect match between BLM and CMM results

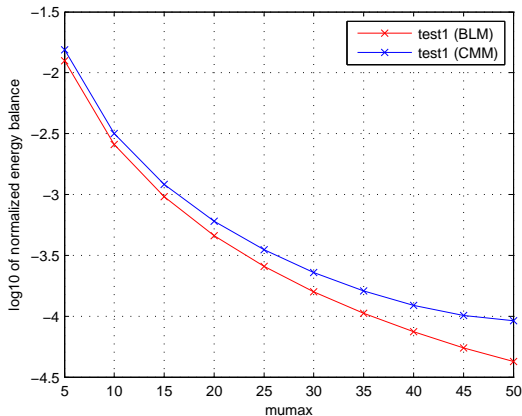
Radial velocity at $r = \{0.035, 0.075, 0.15\}$ m.



Perfect match between BLM and CMM results

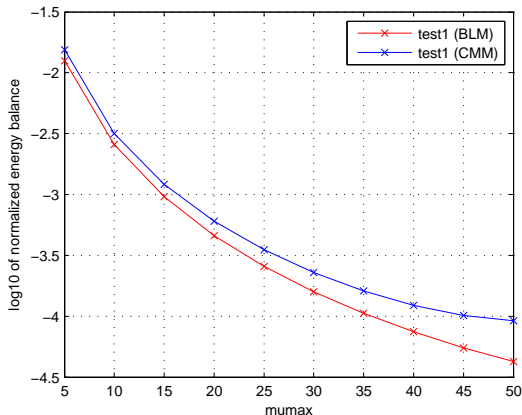
Numerical results — Energy balance

Energy balance (Myers' Energy Corollary) vs μ^{\max} for conf. I



Numerical results — Energy balance

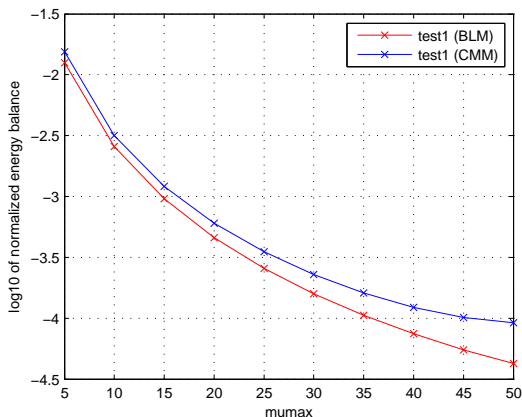
Energy balance (Myers' Energy Corollary) vs μ^{\max} for conf. I



Energy balance better with more μ -modes.

Numerical results — Energy balance

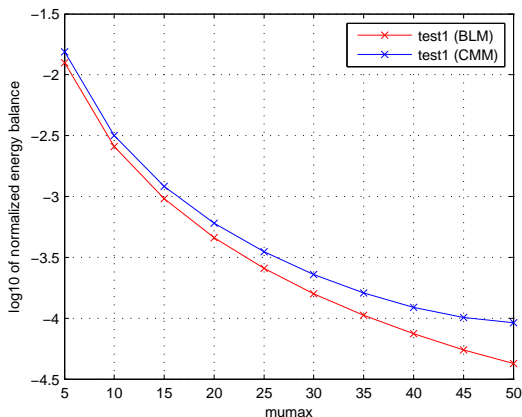
Energy balance (Myers' Energy Corollary) vs μ^{\max} for conf. I



Energy balance better with more μ -modes.
BLM performs better than CMM!

Numerical results — Energy balance

Energy balance (Myers' Energy Corollary) vs μ^{\max} for conf. I



Energy balance better with more μ -modes.
BLM performs better than CMM! Why?

Edge Condition (a posteriori)

Edge Condition (a posteriori)

It is reasonable to assume that for some $p < 0$ the amplitudes

$$A_n = O(n^p) \quad \text{for } n \rightarrow \infty$$

so $\log |A_n| = p \log n + O(1)$.

Edge Condition (a posteriori)

It is reasonable to assume that for some $p < 0$ the amplitudes

$$A_n = O(n^p) \quad \text{for } n \rightarrow \infty$$

so $\log |A_n| = p \log n + O(1)$. Then

$$p_n = \frac{\log |A_n|}{\log n} \rightarrow p \quad \text{for } n \rightarrow \infty$$

Edge Condition (a posteriori)

It is reasonable to assume that for some $p < 0$ the amplitudes

$$A_n = O(n^p) \quad \text{for } n \rightarrow \infty$$

so $\log |A_n| = p \log n + O(1)$. Then

$$p_n = \frac{\log |A_n|}{\log n} \rightarrow p \quad \text{for } n \rightarrow \infty$$

At the interface, at the wall (*edge*): boundary cond. discontinuous.
Field may be singular, but Power Flux must vanish at edge.

Edge Condition (a posteriori)

It is reasonable to assume that for some $p < 0$ the amplitudes

$$A_n = O(n^p) \quad \text{for } n \rightarrow \infty$$

so $\log |A_n| = p \log n + O(1)$. Then

$$p_n = \frac{\log |A_n|}{\log n} \rightarrow p \quad \text{for } n \rightarrow \infty$$

At the interface, at the wall (*edge*): boundary cond. discontinuous.
Field may be singular, but Power Flux must vanish at edge.

It can be shown that:

$$\begin{aligned} p < -1 &\Rightarrow \text{uniform convergence of modal series} \\ &\Rightarrow \text{edge condition satisfied} \end{aligned}$$

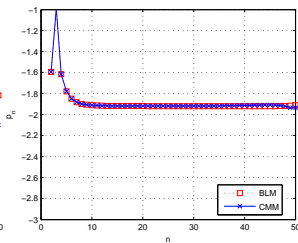
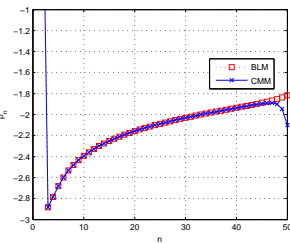
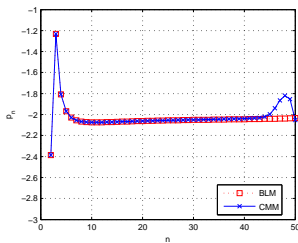
Numerical results — Convergence of modal amplitudes

Do we have $p < -1$ for numerical solutions?

Numerical results — Convergence of modal amplitudes

Do we have $p < -1$ for numerical solutions?

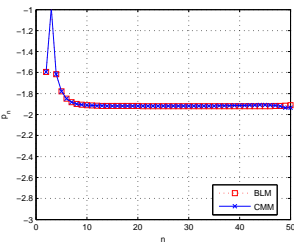
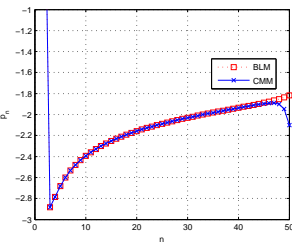
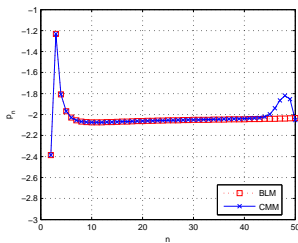
Convergence of amplitudes (BLM and CMM), for conf. I, II and III



Numerical results — Convergence of modal amplitudes

Do we have $p < -1$ for numerical solutions?

Convergence of amplitudes (BLM and CMM), for conf. I, II and III

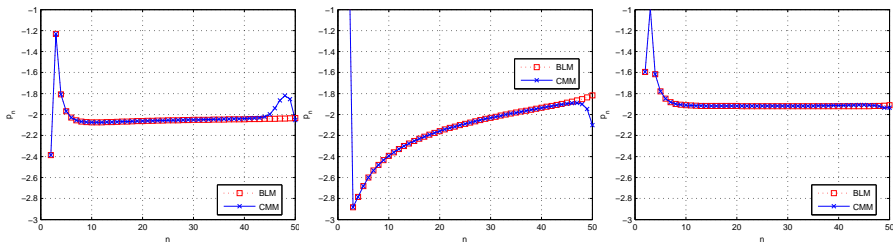


$p \approx -2 \Rightarrow$ edge condition satisfied ✓

Numerical results — Convergence of modal amplitudes

Do we have $p < -1$ for numerical solutions?

Convergence of amplitudes (BLM and CMM), for conf. I, II and III



$p \approx -2 \Rightarrow$ edge condition satisfied ✓

Convergence of p_n reveals inaccuracies of CMM amplitudes:

BLM amplitudes smoother than CMM as $n \rightarrow \infty$: no quadrature inaccuracies for BLM. Explains energy behaviour.

- 1 Background & motivation
- 2 Pridmore-Brown modes
 - Model & equations
 - Numerical method: COLNEW and path-following
- 3 Options for varying Z
- 4 WKB for slowly varying Z
- 5 New mode-matching method
 - Mode-matching basics
 - Closed-form integrals of Helmholtz modes
 - Closed-form integrals of radial Pridmore-Brown modes
 - Mode-matching based on closed form integrals of PB modes
 - Numerical results: comparing CMM and BLM
- 6 Conclusions
 - Epilogue

The *Pridmore-Brown equation* was solved numerically

- Using standard BVP solver COLNEW
- Path-following/predictor-corrector with automatic step size
- Favourable comparison with high-frequency approximation

The *Pridmore-Brown equation* was solved numerically

- Using standard BVP solver COLNEW
- Path-following/predictor-corrector with automatic step size
- Favourable comparison with high-frequency approximation

Slowly varying mode-approximation applied to typical APU duct

- Small enough ε : favourable comparison with BAHAMAS (mode matching)
- WKB fails when Helmholtz liner passes resonance
- Strong effects of temperature and mean flow gradients.
- The need for Mode Matching was clear

Classic mode-matching (CMM):

Classic mode-matching (CMM):

- Uniform flow & temp:
 - Mode shapes are Bessel functions
 - Inner products are available in closed form

Classic mode-matching (CMM):

- Uniform flow & temp:
 - Mode shapes are Bessel functions
 - Inner products are available in closed form
- Parallel (non-uniform) flow & temp:
 - Mode shapes are Pridmore-Brown solutions (determined numerically)
 - Inner products require numerical quadrature
 - expensive & less accurate

Classic mode-matching (CMM):

- Uniform flow & temp:
 - Mode shapes are Bessel functions
 - Inner products are available in closed form
- Parallel (non-uniform) flow & temp:
 - Mode shapes are Pridmore-Brown solutions (determined numerically)
 - Inner products require numerical quadrature
 - expensive & less accurate

Bilinear map-based mode-matching (BLM):

Classic mode-matching (CMM):

- Uniform flow & temp:
 - Mode shapes are Bessel functions
 - Inner products are available in closed form
- Parallel (non-uniform) flow & temp:
 - Mode shapes are Pridmore-Brown solutions (determined numerically)
 - Inner products require numerical quadrature
→ expensive & less accurate

Bilinear map-based mode-matching (BLM):

- Parallel (non-uniform) flow & temp:
 - Mode shapes are Pridmore-Brown solutions (determined numerically)
 - Closed form expressions for “inner-products” cheaper
 - Solutions in very good agreement with CMM
 - BLM amplitudes more accurate

Epilogue

Epilogue

- The success of the BLM matching method is, in a way, too good. At least far better than expected, because the “inner-product” is not a proper inner-product (unless $u_0 = 0$ or uniform) and we can't be sure that it is able to single out each modal contribution.

Epilogue

- The success of the BLM matching method is, in a way, too good. At least far better than expected, because the “inner-product” is not a proper inner-product (unless $u_0 = 0$ or uniform) and we can't be sure that it is able to single out each modal contribution.
- Nevertheless, from the success we can only conclude that it must be “almost” an inner-product. The modes are all “seen” and distinguished.

Epilogue

- The success of the BLM matching method is, in a way, too good. At least far better than expected, because the “inner-product” is not a proper inner-product (unless $u_0 = 0$ or uniform) and we can't be sure that it is able to single out each modal contribution.
- Nevertheless, from the success we can only conclude that it must be “almost” an inner-product. The modes are all “seen” and distinguished.
- Possibly related to this is the fact that the set of discrete modes is not complete, i.e. not sufficient to construct *any* possible solution. There is a “continuous” spectrum at the locus of $\omega - ku_0(r) = 0$. From the energy result we can conclude that this part is very small.

Epilogue

- The success of the BLM matching method is, in a way, too good. At least far better than expected, because the “inner-product” is not a proper inner-product (unless $u_0 = 0$ or uniform) and we can't be sure that it is able to single out each modal contribution.
- Nevertheless, from the success we can only conclude that it must be “almost” an inner-product. The modes are all “seen” and distinguished.
- Possibly related to this is the fact that the set of discrete modes is not complete, i.e. not sufficient to construct *any* possible solution. There is a “continuous” spectrum at the locus of $\omega - ku_0(r) = 0$. From the energy result we can conclude that this part is very small.
- A fine task in functional analysis remains . . .